Molecular Biology of the Cell
Vol. 20, 2438–2450, May 1, 2009

Prm3p Is a Pheromone-induced Peripheral Nuclear Envelope Protein Required for Yeast Nuclear Fusion

Shu Shen, Cynthia E. Tobery,* and Mark D. Rose

Department of Molecular Biology, Princeton University, Princeton, NJ 08544-1014

Submitted October 2, 2008; Revised February 5, 2009; Accepted March 9, 2009
Monitoring Editor: Tim Stearns

Nuclear membrane fusion is the last step in the mating pathway of the yeast *Saccharomyces cerevisiae*. We adapted a bioinformatics approach to identify putative pheromone-induced membrane proteins potentially required for nuclear membrane fusion. One protein, Prm3p, was found to be required for nuclear membrane fusion; disruption of *PRM3* caused a strong bilateral defect, in which nuclear congression was completed but fusion did not occur. Prm3p was localized to the nuclear envelope in pheromone-responding cells, with significant colocalization with the spindle pole body in zygotes. A previous report, using a truncated protein, claimed that Prm3p is localized to the inner nuclear envelope. Based on biochemistry, immunoelectron microscopy and live cell microscopy, we find that functional Prm3p is a peripheral membrane protein exposed on the cytoplasmic face of the outer nuclear envelope. In support of this, mutations in a putative nuclear localization sequence had no effect on full-length protein function or localization. In contrast, point mutations and deletions in the highly conserved hydrophobic carboxy-terminal domain disrupted both protein function and localization. Genetic analysis, colocalization, and biochemical experiments indicate that Prm3p interacts directly with Kar5p, suggesting that nuclear membrane fusion is mediated by a protein complex.

INTRODUCTION

Nuclear fusion (or karyogamy) is the final step in the fusion of two haploid yeast cells to become a diploid zygote. Mating is initiated by secreted pheromones that trigger a signaling cascade in cells of the opposite type, causing arrest in G1 and the development of mating proficiency (Sprague and Thorner, 1994). The two cells grow in a polarized manner toward each other until they come into contact. The intervening cell walls break down and the plasma membranes fuse, forming a zygote with two nuclei. In *Saccharomyces cerevisiae*, as in other fungi, the nuclear envelope never breaks down. Thus, during mating the nuclear envelopes must fuse to form a diploid nucleus. Karyogamy proceeds in two steps: nuclear congression and nuclear envelope fusion (for review, see Marsh and Rose, 1997).

Nuclear envelope fusion is an example of homotypic fusion, involving two membranes of the same composition. The nuclear envelope is itself composed of two membranes (outer and inner), which must fuse in a coordinated manner. Although the detailed mechanism is not well understood, recently it has been demonstrated that nuclear membrane fusion proceeds in three distinct steps (Melloy *et al*., 2007). After the nuclei are pulled together by microtubules emanating from the spindle pole bodies (SPBs), first the outer membranes fuse, followed by inner membrane fusion, and finally by SPB fusion. It is likely that a fusogenic complex made up of proteins localized near the initial site of fusion is responsible for coordinating some or all of these events.

Three proteins have been found to be strongly required for nuclear membrane fusion: Kar5p, Kar2p, and Kar8p. Kar2p is the yeast BiP/GRP78, a protein of the 70-kDa heat-shock protein family localized in the endoplasmic reticulum (ER) lumen (Normington *et al*., 1989; Rose *et al*., 1989). Kar2p performs several functions in mitotic cells, including protein translocation into the ER, folding of secretory proteins, and transport of misfolded proteins out of the ER for degradation (Vogel *et al*., 1990; Sanders *et al*., 1992; Brodsky and Schekman, 1993; Brodsky *et al*., 1995; Simons *et al*., 1995). The role of Kar2p in nuclear fusion is separate from its role in translocation (Vogel *et al*., 1990). Kar8p/Jem1p is a lumenal DnaJ-homologue that is required for nuclear fusion (Nishikawa and Endo, 1997, 1998; Brizzio *et al*., 1999) and likely interacts directly with Kar2p. Overexpression of Kar8p suppresses the mating defect of *kar2-1* (Brizzio *et al*., 1999). Mutations affecting several other proteins that interact with Kar2p (Sec63p, Sec71p/Kar7p, and Sec72p) also cause mild or temperature-sensitive nuclear fusion defects (Ng and Walter, 1996). Last, Kar5p is a novel pheromone-induced integral membrane protein localized to the nuclear envelope near the SPB (Beh *et al*., 1997). Protease protection (Beh *et al*., 1997) and His4C hybrid experiments (Erdeniz and Rose, unpublished observations) demonstrated that the bulk of Kar5p resides within the lumen of the nuclear envelope.

Given that Kar2p, Kar8p, and most of Kar5p reside within the nuclear envelope (NE)/ER lumen, it is unlikely that they would act directly in the initial steps of outer nuclear envelope fusion. Similar to other membrane fusion events, we expect that the initial events would be mediated by proteins such as soluble *N*-ethylmaleimide-sensitive factor attachment protein receptors (SNAREs), anchored on the cytoplasmic face of the nuclear envelope by a transmembrane domain with the bulk of the protein facing outward (for

This article was published online ahead of print in *MBC in Press* (http://www.molbiolcell.org/cgi/doi/10.1091/mbc.E08–10–0987) on March 18, 2009.

* Present address: Dartmouth Center for the Advancement of Learning (DCAL), 102 Baker-Berry Library, HB 6247, Hanover, NH 03755.

Address correspondence to: Mark D. Rose (mdrose@princeton.edu).

Abbreviations used: SPB, spindle pole body.

review, see Burri and Lithgow, 2004). Accordingly, we extended a strategy used by Heiman and Walter (2000) to identify genes encoding putative membrane proteins that are specifically induced during the pheromone response. Examination of disruptions in these genes identified one, *PRM3*, which is strongly required for nuclear fusion during mating. Previous work (Beilharz *et al*., 2003) suggested that Prm3p is an integral membrane protein on the inner nuclear membrane envelope. Instead, we show that Prm3p is a peripheral membrane protein residing on the cytoplasmic face of the nuclear envelope.

MATERIALS AND METHODS

Strains and General Yeast Methods

Yeast media preparation and general yeast methodology was done as described previously (Rose *et al*., 1990; Adams *et al*., 1997). Transformation of yeast was done using the TRAFO method (Gietz and Woods, 2002). Limited plate and filter matings were performed as described previously (Gammie and Rose, 2002). Equal numbers of *MAT***a** and *MAT*α cells were mixed together on a 0.45-μm nitrocellulose filter and allowed to mate for 2.5 h on an YPD plate. Mating mixtures were fixed in 3:1 methanol:acetic acid and stained with 1 μg/ml 4′,6′-diamidino-2-phenylindole (DAPI). The number of nuclei in each zygote was counted to determine the presence of a karyogamy defect. Shmoos were obtained by inducing cells in early exponential phase with 10 μg/ml α-factor for 1.5–2 h.

All strains used are listed in Table 1. All strains are isogenic to S288C. Indicated *MAT***a** and *MAT*α *KanMX* marked deletion strains were obtained from Open Biosystems (Huntsville, AL). The *PRM3* gene disruption was constructed in a diploid strain (MS1556 × MS2290) by a polymerase chain reaction (PCR)-based gene disruption method using *HIS3* as the selective marker (Baudin *et al*., 1993). The gene disruption in the His^+ transformants was confirmed by PCR. Diploids containing the *PRM3* disruption were sporulated and dissected. MS7590, MS7591, MS7592, MS7593, MS7594, and MS7595 are all haploid strains derived from the diploid transformants. Plasmids pMR5062, pMR5063, pMR5064, and pMR5065, carrying various tagged forms of *PRM3*, were constructed using primers designed to generate a product with regions of homology for in vivo recombination (Ma *et al*., 1987). In general, purified PCR products and linearized vector plasmids were cotransformed into yeast. Plasmids from Leu^+ transformants were recovered from yeast, transformed into *Escherichia coli*, and checked by restriction digest and/or PCR.

The *dut ung* site-directed mutagenesis method was used to produce the N-terminal point mutations (Kunkel, 1985). Oligonucleotides used for mutagenesis were designed with 10 base pairs of homology on each side of the mutated residue, with each mutated codon changed to alanine. N-terminal, C-terminal, and internal deletions of *PRM3* were made using in vivo recombination. PCR primers were used to generate DNA fragments with the region of interest deleted and regions of homology to the vector pRS415. Gel-purified PCR products and digested vector were transformed into the yeast strain MS7590 for recombination.

PCR Mutagenesis Screen

PCR mutagenesis was performed using 10× error-prone PCR buffer (100 mM Tris-HCl, pH 8.3, 500 mM KCl, 70 mM $MgCl_2$, and 0.1%, wt/vol gelatin), 0.25 mM each dATP and dGTP, 1 mM each dCTP and dTTP, and 0.3 mM final concentration of $MnCl_2$, 50 pmol of each primer (T3 and T7), 10 ng of template DNA (MR5063), and 5 U of *Taq* polymerase (Hoffman-La Roche, Nutley, NJ). One 100-μl reaction was prepared, separated into 10-μl aliquots to run independently, and mixed back together after PCR reactions were complete. The PCR cycle conditions were 94°C for 30 s, 55°C for 1 min, and 72°C for 1 min, repeated for 30 cycles. PCR products were transformed with digested vector (pRS415) into a *prm3*Δ strain (MS7590) for in vivo recombination and plated out. Mutant colonies were mated to a *prm3*Δ (MS7591) lawn for 2.5 h at 23, 30, and 37°C. Colonies unable to mate were selected for further study. Plasmids were isolated from these strains and transformed back into yeast to check whether mutant phenotypes were still present. Plasmids were then sequenced for the specific mutation.

Immunological Techniques

Mutants were checked for proteins levels using Western blotting. Proteins were precipitated using 50% trichloroacetic acid (TCA), separated by SDS-polyacrylamide gel electrophoresis (PAGE), and transferred to nitrocellulose. Blots were blocked in 5% milk in 10 mM Tris-HCl, pH 7.4, 150 mM NaCl, and 0.05% Tween 20. Green fluorescent protein (GFP) was detected with a mixed mouse monoclonal α-GFP at 1:1000 dilution (Hoffman-La Roche), and the FLAG epitope was detected with a mouse monoclonal antibody at 1:2500 dilution (Sigma-Aldrich, St. Louis, MO). Sec22p and Sec34p were detected using affinity-purified rabbit antibodies used at a 1:2000 dilution (gift from Daniel Ungar and Angela Chan, Princeton University, Princeton, NJ). Secondary antibody (anti-mouse-horseradish peroxidase [HRP]; GE Healthcare, Chalfont St. Giles, Buckinghamshire, United Kingdom) was diluted 1:2500 in blocking buffer and visualized with the enhanced chemiluminescence chemiluminescent system (GE Healthcare).

Indirect immunofluorescent staining of fixed cells was performed with modifications as described previously (Rose *et al*., 1990; Adams *et al*., 1997). Cells were fixed with formaldehyde for 30 min at 30°C; spheroplasts were obtained using 10 mg/ml Zymolyase 100T (MP Biomedicals, Aurora, OH) and 5 μl of β-mercaptoethanol for 30 min at 30°C. Mouse monoclonal anti-GFP (Hoffman-La Roche) was used at a 1:50 dilution and mouse monoclonal anti-FLAG (Sigma-Aldrich) was used at a 1:100 dilution in blocking buffer (10 mg/ml bovine serum albumin and 0.1% NaN_3 in phosphate-buffered saline). The secondary antibody goat anti-mouse fluorescein isothiocyanate (FITC) was used at a 1:500 dilution. Cells were stained with DAPI for localization of the nuclei. For colocalization experiments, two primary antibodies, anti-GFP and anti-Tub4p (a gift from Mark Winey, University of Colorado, Boulder, CO), were incubated with sample concurrently. Anti-GFP was used at 1:50 dilutions, and rat anti-Tub4p was used at a dilution of 1:1000. Secondary antibodies, FITC-conjugated anti-mouse and rhodamine-conjugated anti-rabbit, were used at dilutions of 1:500.

Protease Protection and Extraction

Membrane isolation, protease protection, and protein extractions were performed as described by Beh *et al*. (1997). Exponential phase cells were grown to OD_{600} = 0.5 at which time α-factor was added to 10 μg/ml for 2.5 h. Cells were pelleted and washed twice in 10 ml of spheroplast buffer (0.1 M potassium phosphate, pH 6.5, 1.2 M sorbitol, and 1 mM phenylmethylsulfonyl fluoride [PMSF]). To remove the cell walls, cells were resuspended in 10 ml of spheroplast buffer plus 0.5 ml of 10 mg/ml Zymolyase 100,000T and 50 μl of β-mercaptoethanol. After 1 h at 30°C, spheroplasts were centrifuged at 2K rpm in a centrifuge (Beckman Coulter, Fullerton, CA). After two washes with spheroplast buffer, spheroplasts were resuspended in 25 ml of lysis buffer (20% Ficoll 400, 20 mM potassium phosphate, pH 6.5, 1 mM $MgCl_2$, and 1 mM PMSF) and lysed with 25 strokes of a stainless steel Dounce homogenizer. The lysate was chilled on ice for at least 10 min and centrifuged at 2500 × *g* for 5 min in 30-ml Corex tubes in a JA-17 rotor (Beckman Coulter) at 4°C to pellet unlysed cells. The supernatant was then centrifuged twice at 13,000 × *g* first for 5 min and then for 10 min. The supernatant was then diluted fivefold in cold 20 mM potassium phosphate, pH 6.5, 1 mM $MgCl_2$, and 1 mM PMSF, and the membranes were pelleted in 500-ml bottles (Beckman Coulter) or multiple plastic tubes by centrifugation for 10 min at 11,700 × *g* in a JA-14 or JA-17 rotor (Beckman Coulter) at 4°C.

For protease protection experiments, membrane pellets were resuspended in 2 ml of ice-cold protease buffer (0.3 M mannitol, 0.1 M KCl, 50 mM Tris-HCl, pH 7.5, and 1 mM EGTA) and divided into two equal fractions. To one fraction, Triton X (TX)-100 was added to a final concentration of 1%. Before, and at various times after, the addition of proteinase K (final concentration, 0.3 mg/ml), 150-μl aliquots were taken and mixed with 15 μl of 100% TCA. Samples were chilled for an additional 20 min after the last time point. The samples were centrifuged in a microfuge and washed with 90% acetone. Proteins were resolved by 10% SDS-PAGE.

For protein extractions, the membrane pellet was resuspended in 3 ml of buffer. Aliquots were added to 500 μl of 2× extraction buffer to bring the final concentrations to 1 M NaCl, 1% Triton X-100, 1% Triton X-100/Plus/0.5 M NaCl, or 0.1 M Na_2CO_3, pH 11.0. Samples were extracted on ice for 1 h. Extracted proteins were separated from the membranes by centrifugation at 70,000 × *g* (model TL-100 ultracentrifuge and TLA100.2 rotor; Beckman Coulter) for 1 h. Samples were layered on top of 200 μl of 10% sucrose cushions made in each extraction buffer. Supernatants were removed and precipitated with TCA. Proteins were boiled in sample buffer, and equivalent volumes of pellet and supernatant were separated by 10% SDS-PAGE.

Immunoprecipitation

Lysates for coimmunoprecipitations were prepared as described previously (Jaspersen *et al*., 2006). Mid-log phase cells (100 ml) were treated with α-factor for 1.5 h. Cells were harvested, washed, and resuspended in 1 ml of spheroplast buffer (50 mM Tris-HCl, pH 7.5, 1.2 M sorbitol, and 10 mM NaN_3). Spheroplasts were prepared by treatment with 100 μl of Zymolyase 100T (2.5 mg/ml stock) and 5 μl of β-mercaptoethanol for 30 min at 30°C. Spheroplasts were washed three times in spheroplast buffer, resuspended in lysis buffer (20 mM HEPES-KOH, pH 7.4, 100 mM K-acetate, 5 mM Mg-acetate, 1 mM EDTA, and 1 mM PMSF), and lysed by Dounce homogenization. For cross-linking experiments, extracts were treated with dithiobis(succinimidyl propionate) (0.2 mg/ml) for 10 min on ice and quenched by addition of 50 mM Tris-HCl, pH 8.0. Lysates were centrifuged (11,000 × *g*; 10 min; 4°C), and pellets were resuspended in immunoprecipitation (IP) lysis buffer (50 mM Tris-HCl, pH 7.5, 150 mM NaCl, 5 mM EDTA, and 1% NP-40) to solubilize proteins. The clarified supernatant was taken for immunoprecipitation.

Immunoprecipitations were performed by incubating lysates with either 60 μl of anti-FLAG M2 agarose (Sigma-Aldrich) or 30 μl of Dynabeads protein G (Invitrogen, Carlsbad, CA), with 1:400 dilution anti-hemagglutinin (HA) for 3 h at 4°C. Beads were washed three times in IP lysis buffer and boiled in 100 μl of 2× sample buffer (90 mM Tris-HCl, pH 6.8, 20% glycerol, 2% SDS, 0.02%

Table 1. Strains and plasmids

Strain	Genotype	Source
MS7590	*MAT***a** *prm3Δ::HIS ura3-52 leu2-3.112 his3Δ200 trp1Δ1*	This study
MS7591	*MATα prm3Δ::HIS ura3-52 leu2-3.112 his3Δ200 ade2-101*	This study
MS7592	*MAT***a** *ura3-52 leu2-3.112 his3Δ200 trp1Δ1*	This study
MS7593	*MATα ura3-52 leu2-3.112 his3Δ200 ade2-101*	This study
MS7559	MS7590 with [*GFP-PRM3 LEU2 CEN4 amp-r*]	This study
MS7860	MS7590 with [*GFP-prm3-1 LEU2 CEN4 amp-r*]	This study
MS7861	MS7590 with [FLAG-*prm3-1 LEU2 CEN4 amp-r*]	This study
MS7862	MS7590 with [FLAG-*prm3-2 LEU2 CEN4 amp-r*]	This study
MS7863	MS7590 with [FLAG-*prm3-3 LEU2 CEN4 amp-r*]	This study
MS7864	MS7590 with [*GFP-prm3-4 LEU2 CEN4 amp-r*]	This study
MS7865	MS7590 with [FLAG-*prm3-4 LEU2 CEN4 amp-r*]	This study
MS7866	MS7590 with [FLAG-*prm3-5 LEU2 CEN4 amp-r*]	This study
MS7867	MS7590 with [*GFP-prm3-6 LEU2 CEN4 amp-r*]	This study
MS7868	MS7590 with [*GFP-prm3-7 LEU2 CEN4 amp-r*]	This study
MS7869	MS7590 with [*GFP-prm3-8 LEU2 CEN4 amp-r*]	This study
MS7870	MS7590 with [FLAG-*prm3-10 LEU2 CEN4 amp-r*]	This study
MS7871	MS7590 with [FLAG-*prm3-11 LEU2 CEN4 amp-r*]	This study
MS7872	MS7590 with [FLAG-*prm3-12 LEU2 CEN4 amp-r*]	This study
MS7873	MS7590 with [FLAG-*prm3-13 LEU2 CEN4 amp-r*]	This study
MS7874	MS7590 with [FLAG-*prm3-14 LEU2 CEN4 amp-r*]	This study
MS7875	MS7590 with [FLAG-*prm3-15 LEU2 CEN4 amp-r*]	This study
MS7876	MS7590 with [FLAG-*prm3-16 LEU2 CEN4 amp-r*]	This study
MS7877	MS7590 with [FLAG-*prm3-17 LEU2 CEN4 amp-r*]	This study
MS7878	MS7590 with [FLAG-*prm3-nls LEU2 CEN4 amp-r*]	This study
MS7879	MS7590 with [*GFP-prm3-NΔ LEU2 CEN4 amp-r*]	This study
MS7880	MS7590 with [*GFP-prm3-IΔ LEU2 CEN4 amp-r*]	This study
MS7881	MS7590 with [*GFP-prm3-I2Δ LEU2 CEN4 amp-r*]	This study
MS7882	MS7590 with [*GFP-prm3-I3Δ LEU2 CEN4 amp-r*]	This study
MS7883	MS7590 with [*GFP-prm3-CΔ LEU2 CEN4 amp-r*]	This study
MS7884	*MAT*a *prm3Δ::HIS SPC42:mRFP-kanMX6 ura3-52 leu2-3,112 his3Δ200 trp1Δ1, ade2-101*	This study
MS7885	*MATα prm3Δ::HIS SPC42:mRFP-kanMX6 ura3-52 leu2-3,112 his3Δ200 trp1Δ1, ade2-101*	This study
MS7892	MS7590 with [*GFP-HDEL TRP1 CEN4 amp-r*]	This study
MS7893	MS7884 with [*GFP-HDEL TRP1 CEN4 amp-r*]	This study
MS7816	*MATα PAP1:mRFP-kanMX6 his3d200, ura3-52, leu2-3,112, ade2-101, trp1d1*	Rose laboratory
MS23	*MATα, trp1-Δ1, lys2-801, ade2-101*	Rose laboratory
MS1554	*MAT*a, *ura3-52, leu2-3,112, ade2-101, his3-Δ200*	Rose laboratory
MS1000	*MATα, kar2-1, ura3-52, trp1-Δ1*	Rose laboratory
MS3286	*MAT*a, *kar5Δ::URA3, leu2-3,112, ade2-101, ura3-52*	Rose laboratory
MS3289	*MATα, kar5Δ::URA3, trp1-Δ1, ura3-52*	Rose laboratory
MS7896	MS3286 with [*GFP-PRM3 LEU2 CEN4 amp-r*]	This study
MS7638	*MAT*a, *prm3Δ::HIS3, leu2-3,112, ura3-52, his3Δ200, trp1Δ1* with [*FLAG-PRM3 LEU2 CEN4 amp-r*]	This study
MS7639	*MAT*a, *prm3Δ::HIS3, leu2-3,112, ura3-52, his3Δ200, trp1Δ1* with [*GFP-PRM3 LEU2 CEN4 amp-r*]	This study
MS7617	*MAT*a, *SPC42::GFP, leu2-3,112, ura3-52, his3Δ200, trp1Δ1*	This study
MS740	*MATα, kar1-1, ura3-52, leu2-3,112, ade2-101*	Rose laboratory
MS7666	*MAT*a, *kar5-1162, leu2-3,112, ura3-52, his3Δ200, trp1Δ1*	This study
MS7667	*MATα, kar5-1162, leu2-3,112, ura3-52, his3Δ200, ade2-101*	This study
MS7673	*MATα, kar5Δ::HIS, leu2-3,112, ura3-52, his3Δ200, trp1Δ1*	This study
MS7674	*MAT*a, *kar5Δ::HIS, leu2-3,112, ura3-52, his3Δ200, ade2-101*	This study
MY8094	*MAT*a, *prm3Δ::kanMX, leuΔ2, ura3Δ0, his*Δ1, *met15Δ0* with [*pGAL-GFP-PRM3 LEU2 CEN4 amp-r*]	This study
MS7899	*MATa kar5Δ::HIS3 ura3-5 leu2-3,11 his3-Δ200 ade2-101* [*KAR5*::HA *CEN4 LEU2*]	This study
MS7900	*MATa kar5Δ::HIS3 ura3-5 leu2-3,11 his3-Δ200 ade2-101* [*kar5*::HA-*hyd2Δ CEN4 URA3*]	This study
MS7901	*MATa kar5Δ::HIS3 ura3-5 leu2-3,11 his3-Δ200 ade2-101* [*kar5*::HA-*hyd3Δ CEN4 URA3*]	This study

Plasmid	Genotype	Source
pMR5062	*GFP-PRM3 LEU2 CEN4 amp-r*	This study
pMR5063	*FLAG-PRM3 LEU2 CEN4 amp-r*	This study
pMR5065	*PRM3 LEU2 CEN4 amp-r*	This study
pMR5016	*KAR5 2μ LEU2*	This study
pMR5757	*PRM3 2μ URA3 amp-r*	This study
pMR5760	*KAR5 2μ URA3 amp-r*	This study

bromophenol blue, and 0.1 M dithiothreitol). We analyzed 1/80 each of the input lysate and flow-through and one fourth of the bound protein by SDS-PAGE and Western blotting. Primary antibodies were diluted in blocking buffer as follows: 1:1000 mouse monoclonal anti-GFP (Hoffman-La Roche), 1:5000 mouse monoclonal anti-FLAG (Sigma-Aldrich), and 1:2500 mouse anti-HA. Secondary antibody (anti-mouse HRP; GE Healthcare) was diluted 1:2500 in blocking buffer.

Immunoelectron Microscopy (Immuno-EM)

Shmoos expressing GFP-tagged Prm3p were collected on 0.45-μm nitrocellulose filters for fixation. Cells were fixed by cryoimmobilization in liquid nitrogen under high pressure using an EM Pact High Pressure Freezing Unit (Leica Microsystems, Deerfield, IL). The samples were freeze substituted in 0.25% glutaraldehyde and 0.1% uranyl acetate in acetone for 84 h at −85°C,

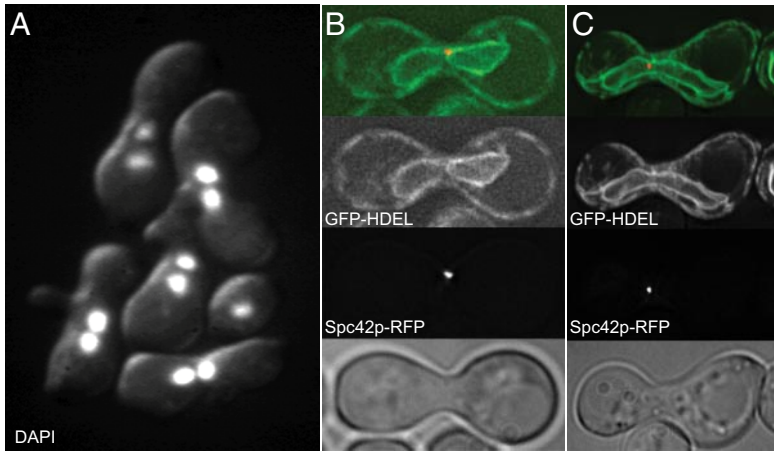

Figure 1. Prm3p is required for nuclear membrane fusion. (A) *prm3*Δ mutant zygotes have closely apposed nuclei (stained with DAPI) that do not fuse (MS7590 × MS7591). (B) *prm3*Δ mutant zygote with 3X-GFP-HDEL expressed around both nuclei. The nuclear membranes are not fused. The first panel shows the GFP-HDEL signal in green and SPC42-RFP, a marker for the spindle pole bodies, in red. The second panel shows GFP-HDEL alone, and the third panel shows SPC42-RFP alone. The fourth panel is a differential interference contrast image of the mutant zygote. (C) Wildtype zygote with 3X-GFP-HDEL expressed in both nuclei. Panels as in (B).

and warmed to −50°C over an 8-h period in an AFS Freeze Substitution Machine (Leica Microsystems). Samples were embedded in Lowicryl HM20 resin at −50°C using UV polymerization. Thin sections of 70 nm were cut on a UC6 ultramicrotome (Leica Microsystems). Sections were probed with mouse monoclonal anti-GFP (Hoffman-La Roche) at a 1:2 dilution for 2 h at room temperature. Secondary antibody was at 1:10 dilution (Ted Pella, Redding, CA) for 2 h at room temperature. Images were observed at 80 kV on a 912AB transmission electron microscope (Carl Zeiss, Thornwood, NY) equipped with an Omega energy filter. Micrographs were captured using a digital camera (Advanced Microscopy Techniques, Danvers, MA).

RESULTS

Identifying Genes Required for Cell or Nuclear Fusion

Many of the genes currently known to be involved in mating are induced by pheromone; moreover, the mechanisms of plasma and nuclear membrane fusion are likely to involve membrane-bound proteins. To identify pheromone-inducible membrane proteins, we extended an approach used by Heiman and Walter (2000) to screen published databases to identify putative pheromone-induced genes with predicted transmembrane domains. To increase the range of potential genes, we identified the set of genes showing at least threefold induction upon exposure to pheromone at various times after treatment (Roberts *et al*., 2000). The presence of transmembrane domains was predicted using the SOSUI program (Hirokawa *et al*., 1998) and TMHMM program (Krogh *et al*., 2001). In total, 55 pheromone-induced genes were predicted to encode transmembrane proteins. Half of the candidates had been characterized previously and were demonstrated to have roles in cell wall synthesis and/or mating, including *PRM1*, *AGA1*, *STE2*, and *FUS1*. The effects of deletions in the 27 remaining genes not described previously as having a role in mating were assayed for potential effects on mating by using a quantitative microscopic mating assay (Gammie *et al*., 1998). This set included six genes identified previously as encoding potential pheromone-induced membrane proteins (Heiman and Walter, 2000). Eight mutants showed a significant cell or nuclear fusion defect (Supplemental Table 1). However, only one deletion mutant exhibited a strong defect (*YPL192C/PRM3*) and was characterized further.

Prm3p Is Required for Nuclear Membrane Fusion

To understand the nature of the mutant phenotype, *prm3* zygotes were examined microscopically for mating defects. Karyogamy mutants are classified as either unilateral or bilateral; unilateral mutants are defective when mated to wild-type cells, bilateral mutants show a defect only when both mating partners are mutant. The *prm3* mutant zygotes showed a strong bilateral karyogamy defect (Figure 1A and Table 2). No defect was apparent in unilateral matings, indicating that Prm3p need be expressed in only one cell for nuclear fusion to occur (Table 2). The nuclear fusion defect in *prm3* mutant zygotes was complemented by a plasmid carrying a copy of *PRM3*, as well as N-terminal FLAG and GFP-tagged *PRM3* (Table 2). Epitope tags at the C terminus of Prm3p resulted in nonfunctional constructs, indicating that the C terminus is important for protein function.

The close apposition of the nuclei in *prm3* zygotes is consistent with a class II nuclear fusion defect (Kurihara *et al*., 1994), in which the nuclei have congressed but nuclear envelope fusion is blocked. To detect a defect in membrane fusion, we examined *prm3* zygotes in which the nuclear envelope lumen was labeled with 3XGFP-HDEL and the spindle pole bodies were labeled with Spc42p-red fluorescent protein (RFP) (Melloy *et al*., 2007). Consistent with a defect in nuclear envelope fusion, the two spindle bodies moved close together, but distinct nuclear envelopes remained surrounding the two unfused haploid nuclei (Figure 1B). In wild-type zygotes, the nuclear envelopes fuse quickly to form a diploid nucleus (Figure 1C). We conclude that Prm3p is required for nuclear envelope fusion.

Table 2. *prm3* is a unilateral karyogamy mutant

Cross	% WT
WT × WT	94
WT × *prm3*Δ	91
*prm3*Δ × *prm3*Δ	6
*prm3*Δ [*PRM3*] × *prm3*Δ	72
*prm3*Δ [GFP-*PRM3*] × *prm3*Δ	68
*prm3*Δ [FLAG-*PRM3*] × *prm3*Δ	73

Matings were performed at 30°C for 2.5 h on nitrocellulose filters on YEPD plates, fixed in 3:1 methanol:acetic acid, and stained with DAPI to visualize the nuclei. Zygotes with one nucleus were counted as Kar^+, whereas zygotes with two nuclei were counted as Kar^-. The percent WT number is the percentage of zygotes that are Kar^+ over total. Numbers represent the average of at least two independent experiments, with ~100 zygotes counted in each experiment. The strains used were *prm3* (MS7590 × MS7591) and WT (MS7592 × MS7593), and the plasmids were MR5062, MR5063, and MR5065.

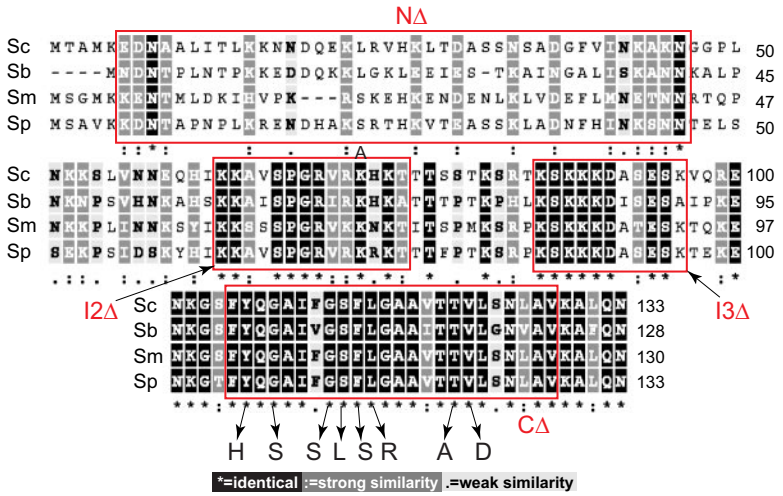

Figure 2. The hydrophobic C-terminal region of Prm3p is highly conserved. (A) Comparison of the Prm3p protein sequence between *S. cerevisiae*, *Saccharomyces bayanus*, *Saccharomyces mikatae*, and *Saccharomyces paradoxus*. Figure modified from the Fungal Sequence Alignment viewer at the Saccharomyces Genome Database, data from Kellis *et al*. (2003). Light gray indicates weak similarity, dark gray indicates strong similarity, and black indicates identical amino acids. The four deleted regions are indicated by red rectangles. Point mutations isolated by saturation mutagenesis are indicated below the sequence. The mutation in the putative NLS (K73→A) is indicated above the sequence.

Prm3p Is a Pheromone-induced Peripheral Membrane Protein

To understand the role Prm3p plays in nuclear membrane fusion, we investigated its structure, expression, and localization within the cell. Prm3p is a small protein of 133 residues, with a predicted transmembrane domain at the carboxy terminus between residues 107-127. Comparison with homologous genes from related yeast species (Cliften *et al*., 2003; Kellis *et al*., 2003) showed that the carboxy-terminal region of Prm3p is highly conserved (Figure 2). This region includes the sole predicted transmembrane domain. The presence of conserved charged residues spaced three or four residues apart in the amino-terminal region suggested a coiled-coil structure that may interact with other proteins. In the middle of the protein are two small highly conserved regions consisting of positively charged residues (Figure 2).

The upstream region of *PRM3* contains a putative pheromone response element, consistent with its regulation by pheromone. To confirm the results from the genome-wide study of pheromone-induced genes, expression of FLAG-Prm3p in both mitotic and pheromone-treated cells was determined using Western blot analysis. Expression of FLAG-Prm3p was only detected in pheromone-treated cells (Figure 3A), consistent with a role in karyogamy.

Although membrane fusion is typically catalyzed by cytoplasmic proteins, all of the proteins identified previously to be strongly required for nuclear membrane fusion (Kar5p, Kar2p, and Kar8p) are located within the nuclear envelope/ER lumen. Initially predicted to have a single transmembrane domain, Prm3p could be oriented with its amino-terminal domain either exposed to the cytoplasm or contained within the lumen of the membrane. To determine the orientation of Prm3p, membrane fractions isolated from cells expressing FLAG-Prm3p were exposed to exogenous protease with and without detergent. Exposed portions of the protein are sensitive to proteases, whereas proteins contained within the lumen are resistant. The majority of FLAG-Prm3p was sensitive to protease in the absence of detergent (Figure 3B). Kar2p, a lumenal protein, remained resistant to protease, demonstrating that the membranes remained intact throughout the course of the experiment (Figure 3B). Comparison of FLAG-Prm3p and Kar2p levels showed that FLAG-Prm3p was degraded with a half-life of ~3 min. Approximately 15% of the protein was not digested within the course of the experiment, due either to protection within a protein complex or the formation of a small amount of inside-out vesicles that protected a fraction of the protein. After addition of detergent to disrupt the membranes, lumenal proteins became fully accessible to proteases, and both proteins were rapidly degraded. We conclude that the Prm3p is oriented such that it is exposed on the outside of the nuclear envelope and not contained within the lumen.

Protein extraction was performed to determine whether Prm3p is an integral membrane protein. Crude membrane fractions were treated with various reagents to extract Prm3p from the membrane. As controls, we also examined the extraction of Sec34p, a peripheral membrane protein and Sec22p, an integral membrane protein (Figure 3C). Typically, peripheral proteins can be extracted with salt or high pH, which disrupt protein–protein interactions, whereas integral membrane proteins require detergents for extraction. As observed previously, the peripheral protein Sec34p was partially extracted under all conditions, but most strongly by high pH (VanRheenen *et al*., 1999). The integral membrane protein Sec22p was not extracted by either 1 M NaCl or high pH. Sec22p was partially extracted by detergent alone and more completely by detergent plus 1 M NaCl. Unlike Sec22p, Prm3p was substantially extracted by 1 M NaCl and not at all by detergent alone. The partial extraction of Prm3p by 1 M NaCl was similar to Sec34p, and all three proteins were more completely extracted by detergent plus 1 M NaCl (Figure 3C). Unlike Sec34p, Prm3p was not extracted by high pH. However, Prm3p has an isoelectric point of 11.1, and many proteins are not soluble near their isoelectric point. Furthermore, Sec72p, another peripheral ER membrane protein is also not extracted at high pH (Feldheim and Schekman, 1994; Kaiser *et al*., 2002). Together with the protease protection data, the protein extraction data indicate that Prm3p is actually a peripheral membrane protein. Unlike the other proteins required for nuclear membrane fusion, Prm3p seems to reside entirely outside of the ER lumen.

Prm3p Is Localized to the Cytoplasmic Face of the Nuclear Envelope

Prm3p may reside on the cytoplasmic or nuclear face of the nuclear envelope. Fusion of GFP or the FLAG epitope to the N terminus resulted in a fully functional protein (Table 2). Both the GFP fusion (Figures 4–6 and 8) and the FLAG-tagged protein (Figures 6 and 7) localized to the nuclear envelope when expressed in either mating or mitotic cells. Similar localization results for the full-length protein in mitotic cells were reported previously (Beilharz *et al*., 2003).

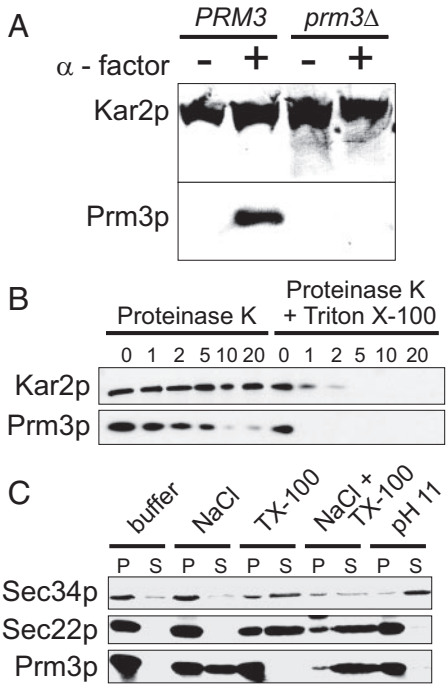

Figure 3. Prm3p is a pheromone-induced peripheral membrane protein. (A) Western blot showing the induction of FLAG-Prm3p upon addition of α-factor. Protein was isolated from cells with (MS7638) or without (MS7590) *FLAG-PRM3*. Blots were probed with anti-FLAG and anti-Kar2 as a loading control. (B) Protease protection experiment showing that Prm3p is not protected in the NE lumen. Membrane fractions from cells expressing *FLAG-PRM3* (MS7638) were treated with proteinase K with or without detergent for 1, 2, 5, 10, and 20 min. Kar2p, residing in the NE lumen, is not degraded in the absence of detergent. Prm3p is completely degraded by the 10-min point. (C) To determine whether Prm3p is a lumenal, integral, or peripheral membrane protein, purified membrane fractions were subjected to various extraction conditions: buffer only; 1 M NaCl, 1% TX-100, 1% TX-100 + 0.5 M NaCl; or 100 mM Na_2CO_3, pH 11. After incubation for 1 h on ice, samples were layered on a sucrose cushion, centrifuged for 1 h at 70,000 × *g* and separated into pellet (P) and supernatant (S) fractions. Blots were probed with anti-FLAG, anti-Sec34, or anti-Sec22 antibodies.

Previously, Prm3p was reported to be a "tail-anchored" integral membrane protein resident on the inner nuclear membrane (Beilharz *et al*., 2003). In that study, GFP was fused to a truncated form of Prm3p lacking the hydrophobic C-terminal domain and was found to localize in the nucleus. Mutation of a putative nuclear localization sequence (NLS) in the truncated protein resulted in mislocalization throughout the cytoplasm. In addition, mutations that disrupt nuclear import (*rna1-1* and *prp20-1*) by failing to regulate the Ran-GTPase caused increased localization of full-length GFP-Prm3p to more peripheral ER (Beilharz *et al*., 2003; King *et al*., 2006). Based on these results, the authors concluded that native full-length Prm3p is an inner nuclear membrane protein. However, localization to the inner nuclear envelope would be surprising, given its role in nuclear envelope fusion. As we show in the next section, the carboxy-terminal region is critical for Prm3p function and its deletion leads to a nonfunctional protein. When the same NLS mutation was introduced into full-length GFP-Prm3p, or the region containing the putative NLS was deleted, the proteins localized to the nuclear envelope (Figure 6F) and supported wild-type levels of nuclear fusion during mating (Figure 6G). Thus, it is unlikely that the putative NLS plays a critical role in Prm3p function. In addition, mutations that affect nuclear import are likely to have a major effect on the localization of many proteins and the mislocalization of Prm3p may result from indirect effects on nuclear structure.

Given its role in nuclear fusion, it is likely that Prm3p is located on the cytoplasmic face of the nuclear envelope. We therefore used two approaches to determine on which face of the nuclear envelope Prm3p resides. Because light microscopy does not provide sufficient resolution to distinguish between the outer and inner nuclear membranes, we used immunoelectron microscopy to localize GFP-Prm3p in shmoos. GFP-Prm3p was detected with mouse anti-GFP and F(ab')2 anti-mouse conjugated to 10-nm gold particles. Gold particles were enriched in the vicinity of the nuclear envelope, as well as sporadically elsewhere in the cell (Figure 4A). The positions of the gold particles relative to the center of the NE lumen were measured (Figure 4B); positive numbers indicate distances toward the cytoplasm, negative numbers indicate distances toward the nucleus. The maximum distance between a gold particle and the center of the ER lumen should be roughly 50 nm, including the length of the primary and secondary antibodies, Prm3p itself, and distance from the membranes to the center of the lumen. Gold particles >80 nm away from the center of the lumen were not measured and were taken to be background staining. In total, 79 gold particles within 80 nm on either side of the nuclear envelope were observed in 36 different cells. In addition, 104 gold particles whose distance from the NE lumen was >80 nm were observed scattered over the entire cross sections of the cells. We estimate that the region of the nuclear envelope showed ~20-fold enrichment in gold particles. The histogram (Figure 4B) shows that the gold particles were highly enriched in a region centered on the outer nuclear membrane. The number of gold particles located within 50 nm of the center of the NE nuclear envelope was significantly higher on the outer membrane than on the inner nuclear membrane ($p = 0.0022$; chi-square test). Assuming that the particles are symmetrically distributed about the outer membrane, then the excess of gold particles on the inner membrane (11 particles) would constitute no more than ~15% of the total.

For an independent test of Prm3p localization, we used live cell microscopy to measure the relative kinetics of transfer of Prm3p between nuclei during nuclear fusion. Because outer nuclear membrane fusion occurs before inner nuclear envelope fusion (Melloy *et al*., 2007), if Prm3p is located on the cytoplasmic face of the nucleus, then it should transfer to the recipient nucleus before a nucleoplasmic protein is able to transfer. Conversely, if Prm3p is only located on the inner nuclear membrane, then transfer of Prm3p could only occur after inner nuclear membrane fusion, at the same time as the nucleoplasmic protein. For this experiment, time-lapse microscopy was performed on wild-type zygotes in which one parent expressed GFP-Prm3p and the other parent expressed Pap1p-mCherryFP as the nucleoplasmic marker. Images of zygotes were taken at 1-min ($n = 4$) or 30-s intervals ($n = 15$) for 15 min, starting immediately after completion of cell fusion. In the example shown, GFP-Prm3p began to transfer to the recipient nucleus after 4 min, whereas the nucleoplasmic marker did not transfer until after 5 min (Figure 4C). Fluorescence intensity in the recipient nuclei was measured and graphed as a percentage of total fluorescence in the zygotes (Figure 4, D and E). The median delay between GFP-Prm3p and Pap1p-cherryFP transfer at half-maximal transfer was ~45 s ($n = 19$). The median delay for the initial time of entry was ~23 s. In four

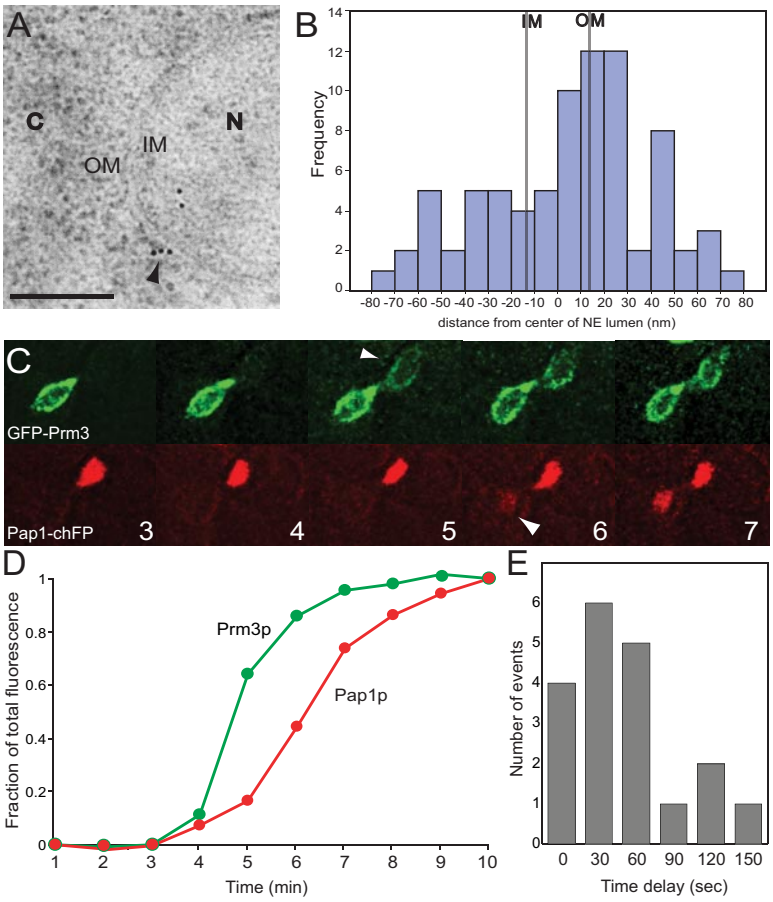

Figure 4. Prm3p is on the cytoplasmic face of the nuclear envelope. (A) Immuno-EM of the nucleus in a shmoo expressing GFP-Prm3p. Cells (MS7590 with MR5062) were induced with α-factor, fixed with high-pressure freezing, embedded in plastic, and sectioned. Samples were labeled with anti-GFP and F(ab')2 anti-mouse conjugated to 10-nm immunogold. (B) Gold particle distance to the center of the NE lumen was measured and graphed on the histogram. Zero (0) indicates the center of the NE lumen. Negative numbers indicate distances to the nuclear side, and positive numbers indicate distances to the cytoplasmic side. Location of outer membrane (OM) and inner membrane (IM) are indicated by dotted lines. (C) Transfer of GFP-Prm3p is detected before transfer of a nucleoplasm marker. Time-lapse microscopy of a zygote with one NE lumen marked by GFP-Prm3p (green) and the other nucleus marked by Pap1-chFP (red). Images were taken at 1-min or 30-s intervals for 15 min. GFP-Prm3p transfers at t = 5 min (arrowhead) and Pap1-chFP transfers at t = 6 min (arrowhead). (D) Fluorescence levels in the recipient nucleus were graphed as a percent of total fluorescence. Time of transfer is extrapolated from taking the slope to the *x*-axis. (E) Histogram of measured time delays from all samples (n = 19).

of 19 zygotes, no delay was observed; transfer of Pap1p-mCherryFP before GFP-Prm3p was not observed. Thus, both the immuno-EM and live cell microscopy demonstrate that Prm3p is primarily located on the cytoplasmic face of the nuclear envelope.

In contrast to the short-term experiments, longer term time-lapse microscopy provided a likely explanation for why *prm3* mutants are bilateral, that is, why Prm3p is not required to be expressed in both mating cells for nuclear fusion to continue. GFP-Prm3p was expressed from the *GAL1* promoter, and cells were mated to a *kar1-1* strain to prevent nuclear congression. Matings were performed on glucose media to shut off synthesis of GFP-Prm3p. As expected, GFP-Prm3p was restricted to one nucleus immediately after cell fusion. After 30 min, GFP-Prm3p was detected on the other nucleus, eventually reaching comparable levels (Figure 5A). By 60 min, the zygote has reentered the mitotic cycle, and two nuclei have moved together near the incipient bud. Thus, one explanation for the *prm3* bilateral phenotype is that Prm3p is only needed in one partner because the protein can shuttle between the two nuclei. Interestingly, when GFP-Prm3p was expressed from the *GAL1* promoter in mitotic cells before mating, it caused striking alterations in the shape of the nuclear envelope (Figure 5B), possibly indicating a role for Prm3p in the structure of the nuclear membranes during karyogamy.

The C-Terminal Region of Prm3p Is Required for Function, Stability, and Localization

To identify the regions of Prm3p required for nuclear envelope-specific localization and function, we analyzed the effects of point and deletion mutations in the gene. To start, we conducted an in vitro mutagenesis screen of *PRM3* to identify point mutations that cause defects in mating. *GFP-PRM3* and FLAG-*PRM3* on centromere plasmids were mutagenized using error-prone PCR, transformed into a *prm3*Δ strain, and the transformants were mated to a *prm3*Δ strain

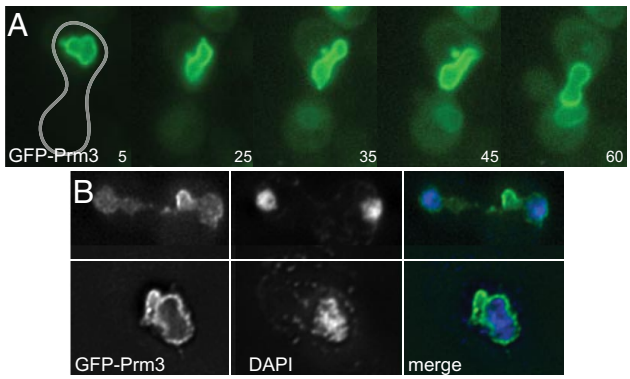

Figure 5. Prm3p Shuttles Between Nuclei. (A) Time-lapse microscopy of GFP-Prm3p in a *kar1-1* zygote. Microscopy began 90 min after mixing **a** and α cells; images were taken every 5 min. Fluorescence can be seen the second nucleus at t = 35 min. (B) Two samples of galactose induced GFP-Prm3p in mitotic cells resulting in proliferation of the nuclear envelope. The first panel is GFP-Prm3p, the second panel is the nucleus stained with DAPI, and the third panel is the merge. Cells were induced with galactose 2 h before fixation for immunofluorescence.

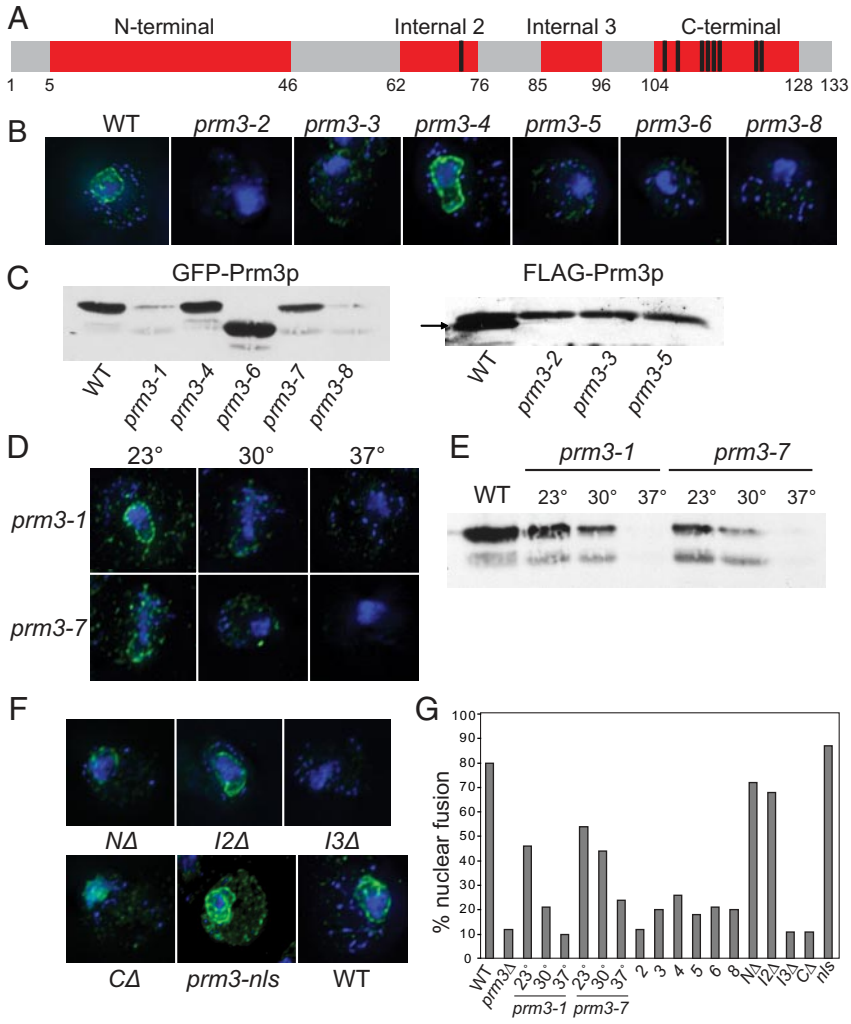

Figure 6. Point mutations in the C terminus affect protein function and localization. (A) Diagram depicting point mutations and deletions in Prm3p. Deletions of the N terminus, the C terminus, and two charged conserved regions in the interior of the protein are indicated in red. Point mutants are highlighted with black stripes. Localization of GFP- or FLAG-tagged Prm3p is shown in B–E. (B) Examples of localization defects seen in *prm3* point mutants. (C) Protein levels of the same point mutants are shown in Western blots. (D) Localization and (E) proteins levels of temperature-sensitive point mutants at 23, 30, and 37°C. (F) Localization of Prm3p in deletion mutants and the *prm3-nls* mutant. (G) Nuclear fusion efficiency of *prm3* point mutants and deletion mutants.

at 23, 30, and 37°C to identify mutants unable to form diploids. Eight point mutations (indicated in Figures 2 and 6A and Table 3) were identified, all located within the conserved hydrophobic C-terminal region. Two point mutations caused temperature-sensitive defects, losing nuclear fusion function at 37°C; growth and cell fusion were not affected. Thirteen nonsense mutations were identified by sequencing and not studied further.

All eight point mutations affected the function, stability, and localization of Prm3p to different extents. Nuclear fusion efficiency decreased to 10–25% of wild type (Figure 6G). Protein levels in *prm3-1*, *prm3-2*, *prm3-3*, *prm3-5*, and *prm3-8* strains were greatly decreased (Figure 6C). Prm3p was mislocalized in *prm3-2*, *prm3-3*, *prm3-5*, *prm3-6*, and *prm3-8* cells (Figure 6B). Mislocalization of the mutant protein and decreased protein levels were correlated, except for mutant *prm3-6*, in which the protein ran at a lower molecular weight. Only in mutant *prm3-4* was the protein stable and localized normally.

Two point mutants, *prm3-1* and *prm3-7*, were temperature sensitive. In both strains, protein function was only slightly reduced at 23°C; nuclear fusion efficiency decreased with increased temperature (Figure 6G). Protein levels in both mutants decreased and Prm3p became increasingly mislocalized with increased temperature (Figure 6, D and E). However, Prm3p became mislocalized in the *prm3-7* mutant at a lower temperature; some mislocalization was seen at 23°C. The presence of stable but mislocalized protein at 23°C suggests that mislocalization of the Prm3p protein by itself does not lead to destabilization. The isolation of point mutations causing defects in nuclear fusion only in the conserved C-terminal region underscores the essential role of this part of the protein for stability, localization, and function.

We used a directed mutagenesis approach to probe the function of the other conserved regions of Prm3p. For example, each of the conserved charged residues in the N-terminal region suggestive of a coiled-coil structure were changed to alanine (Figure 2 and Table 3, *prm10-prm17*); none affected Prm3 function, localization, or stability (data not shown). Because it was possible that multiple residues would need to be mutagenized to cause a defect in function or localization, a deletion of the entire N terminus (residues 1-46) was constructed. Deletion of the N-terminal region (*N*Δ) had no affect on protein function, stability, or localization (Figure 6, F and G). The internal section of Prm3p contains two conserved regions largely made up of positively charged residues. Deletion of region I3 (residues 86-96) had a significant effect on nuclear fusion efficiency and protein stability (Figure 6, F and G). Deletion of region I2 (residues 63-76), which includes the putative NLS sequence, had no effect on function or localization (Figure 6, F and G).

Table 3. *prm3* mutations

Allele	Mutated or deleted residue(s)
prm3-1	108 G to S
prm3-2	122 V to D
prm3-3	114 F to S
prm3-4	113 S to L
prm3-5	115 L to R
prm3-6	121 T to A
prm3-7	106 Y to H
prm3-8	112 C to S
prm3-10	6 E to A
prm3-11	7 D to A
prm3-12	15 K to A
prm3-13	22 K to A
prm3-14	27 K to A
prm3-15	30 D to A
prm3-16	34 N to A
prm3-17	37 D to A
prm3-nls	73 K to A
*prm3-N*Δ	Deleted residues 5-46
*prm3-I*Δ	Deleted residues 46-104
*prm3-C*Δ	Deleted residues 104-128
*prm3-I2*Δ	Deleted residues 63-76
*prm3-I3*Δ	Deleted residues 87-95

As expected, deletion of the C-terminal region (residues 104-128) had severe affects on protein function and localization. Together, the mutational analysis indicates that the C-terminal half of Prm3p is the most critical part of the protein, responsible for function, localization, and stability.

Prm3p Is Concentrated at the SPB and Interacts with Kar5p

Although Prm3p localized to the nuclear envelope in shmoos, immunofluorescent detection of both FLAG-Prm3p and GFP-Prm3p showed distinctly nonuniform staining. In 78% of shmoos, one or more concentrated dots of Prm3p staining were present along the nuclear envelope (Figure 7A). One of the Prm3p dots was adjacent to or colocalized with the SPB in 61% of wild-type shmoos (Figure 7A) and 96% of zygotes (n = 151; Figure 8A). Kar5p, another protein important in karyogamy, is localized adjacent to the SPB (Beh *et al*., 1997). When Kar5p was overexpressed, Prm3p localization at or adjacent to the SPB increased to 93% and Prm3p colocalized with Kar5p in 79% of the shmoos (Figure 7B). Localization of Prm3p to the vicinity of the SPB, the site of nuclear envelope fusion, is consistent with Prm3p's important role in karyogamy.

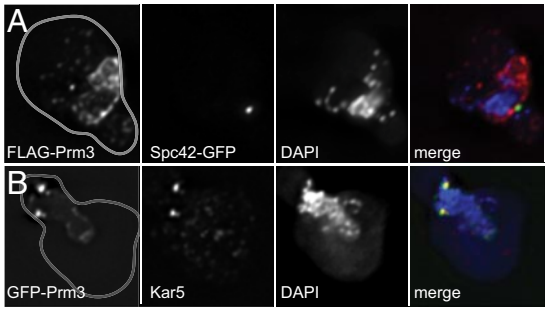

Figure 7. Prm3p is enriched at the SPB. (A) Prm3p shows perinuclear staining with one or more concentrated dots. The first panel shows FLAG-Prm3p localization, the second panel is Spc42-GFP (SPB), the third panel shows the nucleus (stained with DAPI), the fourth panel is the merge. The outline of the shmoo is traced in panel 1. (B) Prm3p colocalizes with Kar5p in 79% of shmoos. The first panel shows GFP-Prm3p, the second panel shows Kar5p, the third panel is the nucleus (stained with DAPI), and the fourth panel is a merge. The shmoo is outlined in panel 1.

The colocalization of Prm3p with Kar5p in shmoos suggested that these proteins may be part of a protein complex that facilitates fusion of the nuclear envelope. To explore the interaction between Prm3p and Kar5p, we examined Prm3p localization in zygotes blocked at the initial stage of nuclear envelope fusion. GFP-Prm3p was enriched at the SPB in 96% (n = 151) of *KAR5* zygotes (Figure 8A). In the *kar5*Δ zygotes, the concentration of GFP-Prm3p at the SPB was reduced (Figure 8B) or disappeared altogether in 29% (n = 96) (Figure 8C). Measurement of the fraction of total GFP-Prm3p at the SPB (Figure 8D) showed that the amount of GFP-Prm3p at the SPB was significantly decreased in the *kar5*Δ zygotes to 54% of wild-type levels ($p = 7 \times 10^{-52}$; Student's *t* test). In contrast, localization of Kar5p to the nuclear periphery was not affected by *prm3*Δ (data not shown). Furthermore, GFP-Prm3p localization in shmoos was not affected by mutations in *KAR7*, *KAR8*, *SEC72*, or *PRM5*. The increased localization of GFP-Prm3p at the SPB when Kar5p is overexpressed in shmoos, together with the decreased localization in *kar5*Δ zygotes, suggests that Kar5p is responsible for recruiting or stabilizing Prm3p to the vicinity of the SPB.

In a second approach to probing the interactions between Kar5p and Prm3p, we examined the genetic interactions between various mutations. Both *prm3*Δ and *kar5*Δ are "bilateral" mutations, requiring both parents to be mutant for nuclear fusion to be defective. When a *prm3*Δ cell was mated to a *kar5*Δ cell, a partial nuclear fusion defect resulted, resulting in 28% Kar^- zygotes (Table 4). This "synthetic" bilateral defect was not observed when *prm3*Δ was mated to other *kar* mutants. A stronger defect was observed when *prm3*Δ was crossed to a partially dominant allele, *kar5-1162*, increasing to 72% (Table 4). Overexpression of Kar5p suppressed the *prm3*Δ nuclear fusion defect; nuclear fusion increased sixfold when *KAR5* was overexpressed in one mating partner and 10-fold when *KAR5* was overexpressed in both mating partners (Table 4). Overexpression of Prm3p did not suppress the mating defect in *kar5*Δ zygotes. Thus, both localization and genetic data suggest that Prm3p interacts with Kar5p.

Prm3p Physically Interacts with Kar5p

To determine whether Prm3p interacts directly with Kar5p, we used coimmunoprecipitation (coIP) of proteins tagged with FLAG, HA, or GFP. Because coIPs of membrane proteins can be complicated by the harsh conditions required to extract the proteins, a membrane permeable cross-linker, dithiobis(succinimidyl propionate) (DSP) was used in some experiments. DSP is a cleavable cross-linker that reacts with the amine group on lysine residues (Walleczek *et al*., 1989). Each experiment was performed with and without DSP; although coprecipitation was detected without the cross-linker, the efficiency was reduced.

When GFP-Prm3p and HA-Kar5p were coexpressed and anti-HA antibody was used to immunoprecipitate HA-Kar5p, a small fraction of the GFP-Prm3p coprecipitated (Figure 9A), consistent with Kar5p's restricted localization near the SPB. As a control, the abundant 3XGFP-HDEL protein in the NE lumen did not coprecipitate with HA-Kar5p. The reciprocal experiment was performed with cells expressing FLAG-Prm3p and HA-Kar5p, by using anti-FLAG antibody to immunoprecipitate FLAG-Prm3p. HA-

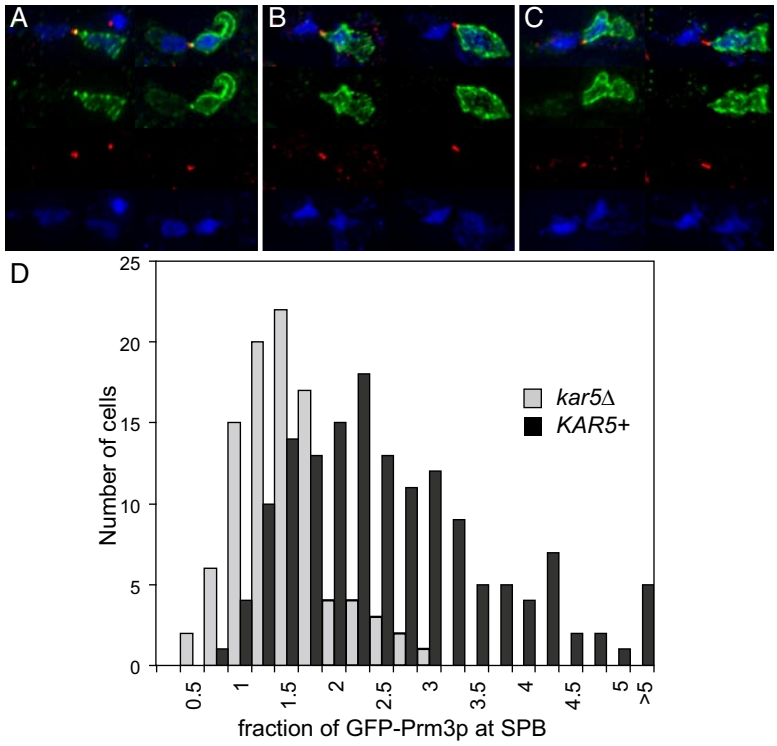

Figure 8. Prm3p localization at the SPB is partially dependent on Kar5p. Coimmunofluorescence of GFP-Prm3, labeled with anti-GFP, and the spindle pole body, labeled with anti-tub4 against γ-tubulin. In A–C, top panels shows a merge of GFP-Prm3p (green), SPB (red), and nuclei stained with DAPI (blue); panels in the second row show GFP-Prm3p; and panels in the third row show the SPBs. Bottom panels show DAPI-stained nuclei. (A) Example of strong enrichment of GFP-Prm3p (green) at the SPB (red) in a *KAR5* zygote. (B) GFP-Prm3p enrichment is reduced at the SPB in a *kar5*Δ zygote. (C) Example of a *kar5*Δ zygote with no GFP-Prm3p enrichment at the SPB. (D) Histogram comparing enrichment of GFP-Prm3p at the SPB in wild-type zygotes (dark gray bars) versus *kar5* mutant zygotes (light gray bars). The *x*-axis is the ratio of GFP fluorescence at the SPB as fraction of total fluorescence in the cells.

Kar5p was coprecipitated with FLAG-Prm3p (Figure 9C), confirming the physical interaction between Prm3p and Kar5p.

The bulk of Kar5p resides within the NE lumen and only ~20 residues between the second and third transmembrane domains are predicted to be exposed to the cytosol (Beh *et al*., 1997; Erdeniz and Rose, unpublished). Thus, the cytosolic loop is the only region of the protein that may be in contact with Prm3p. To determine the role of this region of Kar5p in interactions with Prm3p, coimmunoprecipitations were performed using cells expressing FLAG-Prm3p and HA-tagged *kar5* deletion mutants (Erdeniz and Rose, unpublished). The *kar5-hyd2*Δ mutation is a deletion of the second transmembrane domain, whereas the *kar5-hyd3*Δ mutation is a deletion of the third transmembrane domain (Figure 9B). The topologies of the *kar5* deletion mutant proteins were determined using C-terminal His4C fusions (Sengstag, 2000; Erdeniz and Rose, unpublished). In the *kar5-hyd2*Δ mutant, the third transmembrane domain is oriented such that that the cytosolic loop is within the NE lumen; in the *kar5-hyd3*Δ mutant, the loop remains cytosolic. The mutant proteins were expressed at levels comparable to the wild type (Figure 9C). Comparison of coIPS of the *kar5* mutants with the wild-type strain showed that the amount of Kar5p protein pulled down was significantly reduced in the *kar5-hyd2*Δ mutant (10% wild type) but not in the *kar5-hyd3*Δ mutant (90% wild type; Figure 9C). Therefore, we conclude that the cytosolic loop of Kar5p is required for interaction with Prm3p, consistent with interaction on the cytoplasmic face of the nuclear envelope.

Table 4. *PRM3* and *KAR5* interact genetically

Cross	% WT	% Kar$^-$
WT × *prm3*Δ	97	3
WT × *kar5*Δ	89	11
WT × *kar5*-1162	67	33
*prm3*Δ × *prm3*Δ	6	94
*kar5*Δ × *kar5*Δ	6	94
kar5-1162 × *kar5*-1162	4	96
*prm3*Δ × *kar5*Δ	72	28
*prm3*Δ × *kar5*-1162	28	72
*prm3*Δ × *prm3*Δ	3	97
*prm3*Δ [2μ *PRM3*] × *prm3*Δ	53	47
*prm3*Δ [2μ *PRM3*] × *prm3*Δ [2u *PRM3*]	68	32
*prm3*Δ [2μ *KAR5*] × *prm3*Δ	17	83
*prm3*Δ [2μ *KAR5*] × *prm3*Δ [2u *KAR5*]	32	68

Matings were performed at 30°C for 2.5 h on nitrocellulose filters on YEPD plates, fixed in 3:1 methanol:acetic acid, and stained with DAPI to visualize the nuclei. Zygotes with one nucleus were counted as WT, whereas zygotes with two nuclei were counted as Kar$^-$. Numbers represent the average of at least two independent experiments, with ~100 zygotes counted in each experiment. The strains used were: *prm3* (MS7590 × MS7591), *kar5* (MS7673 × MS7674), and *kar5-1162* (MS7666 × MS7667). Plasmids used were pMR5757 and pMR5760.

DISCUSSION

Prm3p is required for nuclear fusion during mating in *S. cerevisiae*. *PRM3* has several properties that indicate it plays a key role in nuclear fusion during karyogamy. First, *prm3*Δ mutant zygotes have a severe karyogamy defect in which the nuclear membranes fail to fuse. Second, like other proteins important in mating, Prm3p is only expressed in response to pheromone. Third, although Prm3p is localized diffusely over the nuclear envelope, it becomes concentrated

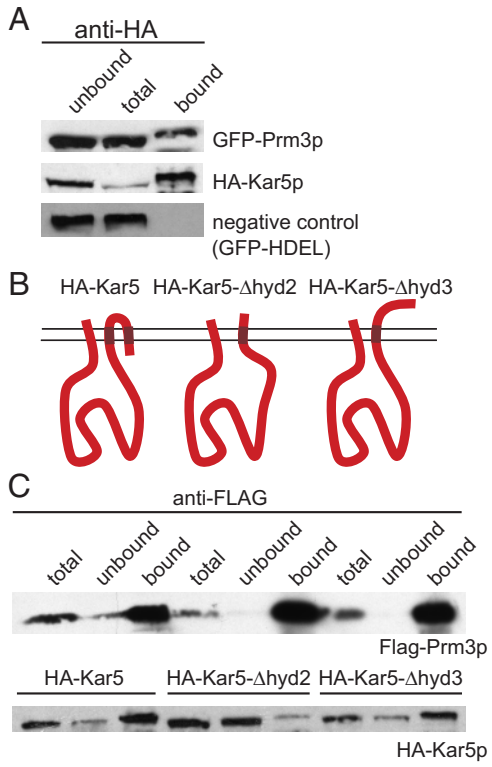

Figure 9. Prm3p interacts with Kar5p. (A) Yeast protein extract containing HA-Kar5p and GFP-Prm3p (MS7590 with pMR2872 and pMR5062) were immunoprecipitated with anti-HA antibody. Total protein (column 1), unbound protein (column 2), and bound protein (column 3) samples were run on SDS-PAGE gels, transferred to nitrocellulose membranes, and blotted with anti-GFP for GFP-Prm3p (top) and anti-HA for HA-Kar5p (middle). Lysate containing GFP-HDEL and HA-Kar5p (MS7592 with pMR2872 and pMR5029) underwent the same IP reaction as a negative control (bottom). (B) Diagram of the topologies of wild-type and mutant Kar5p. Dark red regions indicate the second and third transmembrane domains. (C) Yeast protein extracts from cells expressing FLAG-Prm3p and HA-tagged wild-type or mutant Kar5p (MS7592 with pMR5063 and pMR2872, or pMR5902 and pMR5903) were immunoprecipitated with anti-FLAG antibody conjugated-agarose. Total protein (columns 1, 4, and 7), unbound protein (columns 2, 5, and 8), and bound protein (columns 3, 6, and 9) samples were run on SDS-PAGE gels and blotted with anti-FLAG (top) or anti-HA (bottom). Bands on the Western blots were quantified and the –fold difference between total protein and bound protein calculated.

near the SPB, the initial site of fusion, in shmoos and zygotes. Finally, *PRM3* shows genetic and physical interactions with *KAR5*, which encodes a protein previously shown to play a key role in nuclear fusion.

The role of Prm3p in nuclear envelope fusion leads to an expectation that the protein is located on the cytoplasmic face of the nuclear envelope. Protein extraction experiments demonstrated that Prm3p is a peripheral membrane protein and sensitivity to protease indicates that the amino-terminal FLAG-epitope, at least, is exposed on the surface of the nuclear envelope. Immuno-electron microscopy and live cell microscopy showed that Prm3p resides largely, if not exclusively, on the cytoplasmic face of the nuclear envelope. Based on these data, we conclude that Prm3p resides on the cytoplasmic side of the nuclear envelope, where it can mediate the nuclear membrane fusion.

Localization of Prm3p

A previous study proposed that Prm3p localized to the inner nuclear envelope, based on the nuclear localization of a truncated protein, lacking the hydrophobic carboxy terminus (Beilharz *et al*., 2003). The localization of the truncated protein was mediated by a region of basic residues, similar to a nuclear localization sequence, but which very likely has a different function in the intact protein.

One striking aspect of Prm3p localization is its exclusive localization to the nuclear envelope and not the peripheral endoplasmic reticulum. Restriction to the inner nuclear envelope (Beilharz *et al*., 2003) provided a natural explanation for Prm3p's localization pattern. However, in light of the recognition that Prm3p is a peripheral outer membrane protein, its localization must be governed by interactions with components of the membrane specific to the nuclear envelope. Association with nuclear pore proteins would be one way to restrict Prm3p to the nuclear envelope. For example, Ndc1p, an integral membrane protein, and, Cdc31p, a soluble centrin homologue, are localized to the nuclear envelope at both the SPB and the nuclear pore (Chial *et al*., 1998; Fischer *et al*., 2004). However, except near the SPBs, Prm3p localization is relatively uniform over the surface of the nuclear envelope, making interactions with the nuclear pores less likely. It is, of course, possible that Prm3p localization is dependent on interaction with some other as yet unidentified nuclear membrane specific protein.

Based on its primary sequence, it is tempting to speculate that Prm3p is a lipid binding protein and that nuclear localization is governed by interactions with nuclear-specific lipids. Although it does not share strong homology, Prm3p contains several features similar to many lipid-binding proteins (Cho and Stahelin, 2005). In addition to the extended hydrophobic C-terminal region, Prm3p contains a region significantly enriched in lysines and arginines. In the 28 residues encompassing the two internal conserved regions (I2 and I3), there are 12 lysines and arginines, comparable with the level of charge found in the well characterized phosphatidylinositol bisphosphate (PIP_2) binding myristoylated alanine-rich C-kinase substrate effector domain (13 lysines within 25 residues) PIP_2 (Wang *et al*., 2001). Moreover, the sequence KAVSPGRVRKHK found in region I2 is reminiscent of the conserved PIP_2 binding motif (KATTHEVMGPKKKH found in the adaptin AP180 and related proteins; Ford *et al*., 2001).

The hydrophobic region is predicted to form an amphipathic helix, with all charged and polar residues resident on the one side (Supplemental Figure 1), consistent with a lateral association with the membrane. In general, mutations that disrupt localization changed residues from hydrophobic to polar or charged on the hydrophobic side, and polar residues to hydrophobic on the polar side. Interestingly, mutation *prm3-4*, which changed serine to alanine on the polar side, did not affect localization, suggesting that this part of Prm3p is specifically important for function or protein–protein interaction.

Finally, we note that peripheral membrane proteins often contain aromatic residues that insert into the lipid bilayer (Cho and Stahelin, 2005). When the highly conserved phenylalanine at residue 105 was mutated to either alanine or tyrosine, the mutant protein was nonfunctional and failed to localize (data not shown), suggesting that this residue has a specific function separate from simple hydrophobic interactions. We speculate that Prm3p is a novel lipid-binding protein and that interactions with an as yet unidentified

nuclear envelope-specific lipid may account for its unique localization pattern.

Prm3p Acts at an Early Step of Nuclear Membrane Fusion

The *prm3* mutant zygotes contain nuclei that become closely apposed but do not fuse. Based on Prm3p's localization on the cytoplasmic surface of the nuclear envelope, we predict that Prm3p would act at an early step of nuclear membrane fusion. Electron tomography indicates that Prm3p is required before outer membrane fusion, possibly helping to initiate fusion (Melloy, Shen, White, and Rose, unpublished). Like other membrane fusion events, nuclear fusion is likely to be mediated by SNARE proteins on the nuclear envelope (Burri and Lithgow, 2004), and Prm3p might act as a novel nuclear fusion SNARE or SNARE accessory factor. Superficially, Prm3p resembles a SNARE protein with a region near the N terminus similar to coiled-coils and a hydrophobic domain at the C terminus. However, the N-terminal region is not required for nuclear fusion, making it unlikely that it is acting as a SNARE in this pathway.

Given that such a small region of the protein is essential for nuclear fusion (possibly less than half of the 133 residue protein), the question arises as to what function Prm3p might have in nuclear fusion. Possibly Prm3p interacts with other proteins as part of a fusogenic complex assembled during mating. Alternatively, many peripheral membrane proteins can alter the intrinsic curvature of the membrane (Cho and Stahelin, 2005). Interactions between Prm3p and the nuclear envelope may change the physical properties of the membrane to aid fusion. Consistent with this hypothesis, expression of Prm3p in mitotic cells caused proliferation of curved nuclear membranes.

Prm3p Interacts with Kar5p

Proteins important in nuclear membrane fusion are expected to interact with each other in a fusogenic complex. Localization data suggested that Kar5p helps recruit or stabilize Prm3p at the SPB. Coimmunoprecipitation experiments showed that Prm3p and Kar5p physically interact, most likely through a small region of Kar5p residing outside the NE lumen. *PRM3* and *KAR5* also showed genetic interactions (synthetic bilateral defects and dosage suppression) consistent with their physical interaction. The genetic interactions between *PRM3* and *KAR5* were not reciprocal; overexpression of Kar5p partially suppressed *prm3*Δ, but overexpression of Prm3p did not suppress *kar5*Δ. This result suggests that Prm3p may play an accessory role, enhancing the activity or stability of proteins such as Kar5p that may act more directly in nuclear fusion.

ACKNOWLEDGMENTS

We thank the members of the Rose laboratory for extended discussions. We thank Naz Erdeniz for constructing the *kar5-hyd* deletion mutations. We thank Peggy Bisher for extensive help with the immuno-EM experiments. This work was supported by National Institutes of Health grant GM-37739 (to M.D.R.).

REFERENCES

Adams, A., Gottschling, D. E., Kaiser, C. A., and Stearns, T. (1997). Methods in Yeast Genetics: A Cold Spring Harbor Laboratory Course Manual, Cold Spring Harbor, NY: Cold Spring Harbor Laboratory Press.

Baudin, A., Ozier-Kalogeropoulos, O., Denouel, A., Lacroute, F., and Cullin, C. (1993). A simple and efficient method for direct gene deletion in *Saccharomyces cerevisiae*. Nucleic Acids Res. *21*, 3329–3330.

Beh, C. T., Brizzio, V., and Rose, M. D. (1997). KAR5 encodes a novel pheromone-inducible protein required for homotypic nuclear fusion. J. Cell Biol. *139*, 1063–1076.

Beilharz, T., Egan, B., Silver, P. A., Hofmann, K., and Lithgow, T. (2003). Bipartite signals mediate subcellular targeting of tail-anchored membrane proteins in *Saccharomyces cerevisiae*. J. Biol. Chem. *278*, 8219–8223.

Brizzio, V., Khalfan, W., Huddler, D., Beh, C. T., Andersen, S. S., Latterich, M., and Rose, M. D. (1999). Genetic interactions between *KAR7/SEC71*, *KAR8/JEM1*, *KAR5*, and *KAR2* during nuclear fusion in *Saccharomyces cerevisiae*. Mol. Biol. Cell *10*, 609–626.

Brodsky, J. L., Goeckeler, J., and Schekman, R. (1995). BiP and Sec63p are required for both co- and posttranslational protein translocation into the yeast endoplasmic reticulum. Proc. Natl. Acad. Sci. USA *92*, 9643–9646.

Brodsky, J. L., and Schekman, R. (1993). A Sec63p-BiP complex from yeast is required for protein translocation in a reconstituted proteoliposome. J. Cell Biol. *123*, 1355–1363.

Burri, L., and Lithgow, T. (2004). A complete set of SNAREs in yeast. Traffic *5*, 45–52.

Chial, H. J., Rout, M. P., Giddings, T. H., and Winey, M. (1998). *Saccharomyces cerevisiae* Ndc1p is a shared component of nuclear pore complexes and spindle pole bodies. J. Cell Biol. *143*, 1789–1800.

Cho, W., and Stahelin, R. V. (2005). Membrane-protein interactions in cell signaling and membrane trafficking. Annu. Rev. Biophys. Biomol. Struct. *34*, 119–151.

Cliften, P., Sudarsanam, P., Desikan, A., Fulton, L., Fulton, B., Majors, J., Waterston, R., Cohen, B. A., and Johnston, M. (2003). Finding functional features in *Saccharomyces* genomes by phylogenetic footprinting. Science *301*, 71–76.

Feldheim, D., and Schekman, R. (1994). Sec72p contributes to the selective recognition of signal peptides by the secretory polypeptide translocation complex. J. Cell Biol. *126*, 935–943.

Fischer, T., Rodriguez-Navarro, S., Pereira, G., Racz, A., Schiebel, E., and Hurt, E. (2004). Yeast centrin Cdc31 is linked to the nuclear mRNA export machinery. Nat. Cell Biol. *6*, 840–848.

Ford, M. G., Pearse, B. M., Higgins, M. K., Vallis, Y., Owen, D. J., Gibson, A., Hopkins, C. R., Evans, P. R., and McMahon, H. T. (2001). Simultaneous binding of PtdIns(4,5)P2 and clathrin by AP180 in the nucleation of clathrin lattices on membranes. Science *291*, 1051–1055.

Gammie, A. E., Brizzio, V., and Rose, M. D. (1998). Distinct morphological phenotypes of cell fusion mutants. Mol. Biol. Cell *9*, 1395–1410.

Gammie, A. E., and Rose, M. D. (2002). Assays of cell and nuclear fusion. Methods Enzymol. *351*, 477–498.

Gietz, R. D., and Woods, R. A. (2002). Transformation of yeast by lithium acetate/single-stranded carrier DNA/polyethylene glycol method. Methods Enzymol. *350*, 87–96.

Heiman, M. G., and Walter, P. (2000). Prm1p, a pheromone-regulated multispanning membrane protein, facilitates plasma membrane fusion during yeast mating. J. Cell Biol. *151*, 719–730.

Hirokawa, T., Boon-Chieng, S., and Mitaku, S. (1998). SOSUI: classification and secondary structure prediction system for membrane proteins. Bioinformatics *14*, 378–379.

Jaspersen, S. L., Martin, A. E., Glazko, G., Giddings, T. H., Jr., Morgan, G., Mushegian, A., and Winey, M. (2006). The Sad1-UNC-84 homology domain in Mps3 interacts with Mps2 to connect the spindle pole body with the nuclear envelope. J. Cell Biol. *174*, 665–675.

Kaiser, C. A., Chen, E. J., and Losko, S. (2002). Subcellular fractionation of secretory organelles. Methods Enzymol. *351*, 325–338.

Kellis, M., Patterson, N., Endrizzi, M., Birren, B., and Lander, E. S. (2003). Sequencing and comparison of yeast species to identify genes and regulatory elements. Nature *423*, 241–254.

King, M. C., Lusk, C. P., and Blobel, G. (2006). Karyopherin-mediated import of integral inner nuclear membrane proteins. Nature *442*, 1003–1007.

Krogh, A., Larsson, B., von Heijne, G., and Sonnhammer, E. L. (2001). Predicting transmembrane protein topology with a hidden Markov model: application to complete genomes. J. Mol. Biol. *305*, 567–580.

Kunkel, T. A. (1985). Rapid and efficient site-specific mutagenesis without phenotypic selection. Proc. Natl. Acad. Sci. USA *82*, 488–492.

Kurihara, L. J., Beh, C. T., Latterich, M., Schekman, R., and Rose, M. D. (1994). Nuclear congression and membrane fusion: two distinct events in the yeast karyogamy pathway. J. Cell Biol. *126*, 911–923.

Ma, H., Kunes, S., Schatz, P. J., and Botstein, D. (1987). Plasmid construction by homologous recombination in yeast. Gene *58*, 201–216.

Marsh, L., and Rose, M. D. (1997). The pathway of cell and nuclear fusion during mating in *S. cerevisiae*. In: The Molecular and Cellular Biology of the

Yeast *Saccharomyces*: Cell Cycle and Cell Biology, ed. J.R.B. J. R. Pringle, and E. W. Jones, Cold Spring Harbor, NY: Cold Spring Harbor Laboratory Press, 827–888.

Melloy, P., Shen, S., White, E., McIntosh, J. R., and Rose, M. D. (2007). Nuclear fusion during yeast mating occurs by a three-step pathway. J. Cell Biol. *179*, 659–670.

Ng, D. T., and Walter, P. (1996). ER membrane protein complex required for nuclear fusion. J. Cell Biol. *132*, 499–509.

Nishikawa, S., and Endo, T. (1997). The yeast JEM1p is a DnaJ-like protein of the endoplasmic reticulum membrane required for nuclear fusion. J. Biol. Chem. *272*, 12889–12892.

Nishikawa, S., and Endo, T. (1998). Reinvestigation of the functions of the hydrophobic segment of Jem1p, a yeast endoplasmic reticulum membrane protein mediating nuclear fusion. Biochem. Biophys. Res. Commun. *244*, 785–789.

Normington, K., Kohno, K., Kozutsumi, Y., Gething, M. J., and Sambrook, J. (1989). *S. cerevisiae* encodes an essential protein homologous in sequence and function to mammalian BiP. Cell *57*, 1223–1236.

Roberts, C. J., *et al*. (2000). Signaling and circuitry of multiple MAPK pathways revealed by a matrix of global gene expression profiles. Science *287*, 873–880.

Rose, M. D., Misra, L. M., and Vogel, J. P. (1989). KAR2, a karyogamy gene, is the yeast homolog of the mammalian BiP/GRP78 gene. Cell *57*, 1211–1221.

Rose, M. D., Winston, F., and Hieter, P. (1990). Methods in Yeast Genetics: A Cold Spring Harbor Laboratory Course Manual. Cold Spring Harbor, NY: Cold Spring Harbor Laboratory Press.

Sanders, S. L., Whitfield, K. M., Vogel, J. P., Rose, M. D., and Schekman, R. W. (1992). Sec61p and BiP directly facilitate polypeptide translocation into the ER. Cell *69*, 353–365.

Sengstag, C. (2000). Using SUC2-HIS4C reporter domain to study topology of membrane proteins in *Saccharomyces cerevisiae*. Methods Enzymol. *327*, 175–190.

Simons, J. F., Ferro-Novick, S., Rose, M. D., and Helenius, A. (1995). BiP/Kar2p serves as a molecular chaperone during carboxypeptidase Y folding in yeast. J. Cell Biol. *130*, 41–49.

Sprague, G.F.J., and Thorner, J. W. (1994). Pheromone response and signal transduction during the mating process of *Saccharomyces cerevisiae*. In: The Molecular and Cellular Biology of the Yeast *Saccharomyces*, ed. J.R.P.E.W. Jones and J. R. Broach, Cold Spring Harbor, NY: Cold Spring Harbor Laboratory, 657–744.

VanRheenen, S. M., Cao, X., Sapperstein, S. K., Chiang, E. C., Lupashin, V. V., Barlowe, C., and Waters, M. G. (1999). Sec34p, a protein required for vesicle tethering to the yeast Golgi apparatus, is in a complex with Sec35p. J. Cell Biol. *147*, 729–742.

Vogel, J. P., Misra, L. M., and Rose, M. D. (1990). Loss of BiP/GRP78 function blocks translocation of secretory proteins in yeast. J. Cell Biol. *110*, 1885–1895.

Walleczek, J., Martin, T., Redl, B., Stoffler-Meilicke, M., and Stoffler, G. (1989). Comparative cross-linking study on the 50S ribosomal subunit from *Escherichia coli*. Biochemistry *28*, 4099–4105.

Wang, J., Arbuzova, A., Hangyas-Mihalyne, G., and McLaughlin, S. (2001). The effector domain of myristoylated alanine-rich C kinase substrate binds strongly to phosphatidylinositol 4,5-bisphosphate. J. Biol. Chem. *276*, 5012–5019.